Multi-objective Optimal Allocation of Distributed Generation Considering Environmental Target and Uncertainty of EV

Huazhen Cao, Yaxiong Wu, Chong Gao, Junxi Tang and Lvpeng Chen

Abstract Based on the typical timing characteristics of Distributed Generation (DG) and user power load, considering the uncertainty of large-scale electric vehicles and the environmental benefits of different distributed power sources, the operating cost, network loss and environmental benefit of the distribution network are used as the objective function. In this paper, a Monte Carlo simulation method is used to simulate the charging characteristic of the electric vehicle, and the model is solved by the binary bat algorithm. By comparing with a single-purpose distributed power optimization configuration model, the simulation results verify the rationality and validity of the proposed model and method.

Keywords Distributed generation · Electric vehicle · Time-sequence characteristics of load · Multi-objective bat optimization algorithm

1 Introduction

In order to solve the energy shortage and environmental problems, distributed generation technology and electric vehicle industry are developing rapidly [1–3]. Because the output characteristics of Distributed Generation (DG) are random and

Foundation item: Supported by the Technical Projects of China Southern Power Grid (No. GDKJXM20172939).

H. Cao · Y. Wu · C. Gao · J. Tang
Grid Planning & Research Center, Guangdong Power Grid Co., Ltd., CSG, Guangzhou 510030, China

H. Cao · Y. Wu · C. Gao · J. Tang
Guangdong Power Grid Development Research Institute Co., Ltd., Guangzhou 510030, China

L. Chen (✉)
Suzhou Huatian Power Technology Co., Ltd., Suzhou 215000, China
e-mail: chenlvpeng123@163.com

Y. Xue et al. (eds.), *Proceedings of PURPLE MOUNTAIN FORUM 2019-International Forum on Smart Grid Protection and Control*, Lecture Notes in Electrical Engineering 585, https://doi.org/10.1007/978-981-13-9783-7_18

intermittent, when a large number of DGs connected to the distribution network, it will have a huge impact on the operation of the distribution network.

The charging characteristics of the electric vehicle (EV) have great space-time uncertainty. With the increasing of the permeability of the EV, the existing distribution network will likely have a problem of operation [4]. Therefore, the planner should consider the uncertain characteristics of the DG and the EV in the planning of the DG optimization configuration, so as to be of great significance to the development of the distribution network.

At present, many scholars have done a lot of research on the problem of DG optimal allocation, and have achieved relevant results [5]. The model established in reference [6] takes into account the cost of purchasing electricity, the cost of lack of power, the cost of loss and the cost of delaying network renewal. The random characteristics of DG and PEV under different permeability are considered in reference [7], but the genetic algorithm has the disadvantage that it is easy to fall into precocity.

In this paper, the charging characteristics of EV are modeled, and the timing characteristics of DG and conventional load are analyzed and extracted. The multi-objective DG optimal configuration model is established based on the distribution network loss, the operation cost of DG construction, and the environmental benefit as the objective function. The binary bat algorithm is used to solve the model. The numerical results show that the proposed optimization model and method are effective and flexible.

2 Probabilistic Modeling and Simulation of EV Charging Characteristics

2.1 Behavior Characteristics of EV

According to the results of the American household traffic survey data (NHTS) [8], it is found that the time T of the car owner's last end trip obeys the normal distribution. Its probability density can be expressed as (1):

$$f(T) = \begin{cases} \dfrac{1}{\sqrt{2\pi}\sigma_T}\exp\left[-\dfrac{(T-\mu_T)^2}{2\sigma_T^2}\right], (\mu_T - 12) < T \le 24 \\ \dfrac{1}{\sqrt{2\pi}\sigma_T}\exp\left[-\dfrac{(T+24-\mu_T)^2}{2\sigma_T^2}\right], 0 < T \le (\mu_T - 12) \end{cases} \tag{1}$$

where μ_T= 17.6; σ_T= 3.4.

2.2 Characteristics and Charging Mode of EV's Battery

It is assumed that the battery characteristic parameters adopted in this paper are as follows: the capacity of EV battery is 30 kWh, the initial SOC meets normal distribution **N**(0.5, 0.01) at the beginning of charging. The charging efficiency is 95% and the charging power factor is 0.95. The charging power is assumed to be constant and the charging power is 3.5 kW. The car owner will adopt the disordered charging mode. Suppose the owner's charging time is at the end of the last trip. According to (1) and battery characteristics of electric private car, Monte Carlo simulation method can be used to simulate the charging load characteristics of EV.

3 Time-Sequence Characteristics of DG and Load

3.1 Time-Sequence Characteristics of DG

The output characteristics of Wind turbine generator (WT) and photovoltaic generator (PV) both have volatility and randomness. However, there is a certain regularity within a certain time scale (for example, daily). The typical daily output curves of WT and PV are shown in Fig. 1. The output data of WT and PV are selected from a distributed power plant under heavy load period in Maoming City, Guangdong Province.

It can be seen from the typical output curves that there is a certain complementarity between the output rule of WT and PV. The complementary characteristics between WT and PV naturally smooth the peak-valley difference of distribution system to a certain extent.

Micro-turbine generator (MT)is a widely used distributed generator. Different from WT and PV affected by geographical location and natural conditions, their

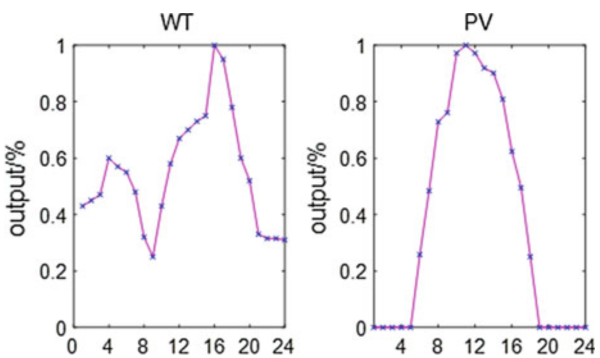

Fig. 1 Typical output curves of WT and PV on July 23, 2018

time series output characteristics are precisely controllable. Therefore, the time series output characteristic is regarded as constant in this paper.

3.2 Extraction Method of Time-Sequence Characteristics of Load

With the continuous development of social economy, especially the emergence of new load, the characteristic difference of electric load time series curve is gradually increasing. DG optimal configuration planning also needs to extract the timing characteristics of the load. In this paper, Fuzzy C-Means (FCM) is selected as the extraction method of load timing characteristics [9].

4 Multi-objective DG Optimal Configuration Model

4.1 Objective Function

Distribution Network Loss Target.

$$C_{\mathrm{L}} = 365 \times price_{\mathrm{loss}} \sum_{N_{\mathrm{T}}}^{N_{\mathrm{T}}} \sum_{l=1}^{N_{\mathrm{L}}} I_{tl}^{2} R_{l} \Delta t \tag{2}$$

where C_{L} is the annual cumulative loss cost after DG is configured, $price_{\mathrm{loss}}$ is the loss price, N_T is the segment number of the time series characteristic curve, this paper takes 24 N_L as the total branch number of the optimized regional distribution network. The I_{tl} is the current on the branch l after the DG is connected to the distribution network, the R_l is the branch resistance of the branch l, and Δt is the time interval.

DG Construction Operation Cost Target. The DG construction operating cost target consists of the DG construction cost $\mathrm{C_{CON}}$ and the operational maintenance cost $\mathrm{C_{OM}}$, as shown in (3):

$$C_{\mathrm{DG}} = \sum_{k=1}^{N_{\mathrm{DG}}} S_k \left[\left(\frac{\eta (1+\eta)^{n_{\mathrm{DG},k}}}{(1+\eta)^{n_{\mathrm{DG},k}} - 1} \right) C_{\mathrm{CON},k} + 8760 C_{\mathrm{OM},k} \right] \tag{3}$$

where N_{DG} is the number of DG in distribution network, η is fixed annual interest rate, unit is %, $n_{\mathrm{DG},k}$ is the repayment period of construction funds, which is equal to the economic operating life of DG, S_k is the planning capacity of the kth DG. $C_{\mathrm{CON},k}$ and $C_{\mathrm{OM},k}$ are the unit capacity construction cost and operation maintenance cost of the kth DG, respectively.

Environmental Benefit Target [10]:

$$C_{\mathrm{E}} = \sum_{k=1}^{N_{\mathrm{DG}}} Q_k \sum_{i=1}^{N_{\mathrm{P}}} \left(C_{\mathrm{F}i} - C_{\mathrm{DG}ki}\right) \tag{4}$$

$$Q_k = 365 \times \sum_{t=1}^{N_T} P_{kt} \Delta t \tag{5}$$

where C_E is the annual environmental benefit after DG is configured, N_{DG} is the number of DG configured in distribution network, Q_k is the annual power generation of the kth DG, N_P is the number of pollutants, and N_{DG} is the number of DG in distribution network. C_{Fi} and C_{DGki} are the environmental value costs of thermal power generation and the *i*th pollutant emitted by the *k*th DG distributed power source, respectively. P_{kt} is the active contribution of the *k*th DG in the t-period of the daily load series.

4.2 Constraint Condition

Power Flow Constraints

$$\begin{cases} P_{is} = U_i \sum\limits_{j \in i} U_j (G_{ij} \cos\theta_{ij} + B_{ij} \sin\theta_{ij}) \\ Q_{is} = U_i \sum\limits_{j \in i} U_j (G_{ij} \sin\theta_{ij} - B_{ij} \cos\theta_{ij}) \end{cases} \tag{6}$$

where P_{is} and Q_{is} are the active power injection power and reactive power injection power of node *i*, respectively, U_i and U_j denote the voltage amplitude of node *i* and node *j*, and $j \in i$ denote all nodes directly connected to node *i*, respectively, and U_i and U_j denote the voltage amplitude of node *i* and node *j*, respectively. G_{ij} and B_{ij} represent conductance and admittance between node *i* and node *j* respectively, θ_{ij} is the phase angle difference between node *i* and node *j*.

Node Voltage Constraint

$$U_i^{\min} \le U_i \le U_i^{\max} \tag{7}$$

where U_i^{min} and U_i^{max} represents the upper and lower limits of the voltage of node i.

Transmission Line Capacity Constraints

$$P_{ij} < P_{ij,\max} \tag{8}$$

where P_{ij} represents the transmitted power from node i to node j.

Total DG Access Capacity Constraint

$$S^{\min} \le \sum_{k=1}^{N_{\mathrm{DG}}} S_k \le S^{\max} \tag{9}$$

where $S_{\min}$ and $S_{\max}$ represents the upper and lower limits of the capacity in a distribution network that allows access to a distributed source.

4.3 Synthetic Objective Function

To sum up, the above three optimization objectives conflict with each other, so the coordination optimization is difficult. Therefore, the weighted variable ω_m is introduced to express the decision preference of different objectives. The synthetic objective function is shown in (10).

$$\min C = \omega_1 C_{\mathrm{L}} + \omega_2 C_{\mathrm{DG}} - \omega_3 C_{\mathrm{E}} \tag{10}$$

where ω_1, ω_2 and ω_3 are the weight coefficients of each objective, and ω_1+ ω_2+ $_3$ = 1. Each weight can be selected according to experience. The more close to 1 the weight coefficient is, the more important it is to consider its corresponding index. This paper mainly considers transmission loss, environmental benefit and DG construction cost as the influencing factors of weight selection.

5 Solution of the Model

5.1 Particle Position Coding Scheme Setting

Particle position information includes the type of access to the DG and the DG access capacity. The encoding method is binary coded, as shown in (11)

$$X = \{K_1, S_1, K_2, S_2, \ldots, K_{N_{\text{bus}}}, S_{N_{\text{bus}}}\} \tag{11}$$

where X is the location information of bats, K_i is the type of DG at distribution node i, and S_i is the capacity of DG at distribution node i.

5.2 *Binary Bat Algorithm*

Bat Algorithm (BA) is a new intelligent optimization algorithm, which is suitable for solving the continuous optimization problem of decision variables. The DG optimization problem is an integer optimization problem, so the standard BA cannot be adopted directly. By modifying the process of updating the speed and position of the BA, the standard BA is transformed into the Binary Bat Algorithm (BBA) to solve the DG optimal configuration problem [11].

The specific process is described as follows:

Step (1): Initializes the BBA algorithm parameters. Set the sound level A, the pulse frequency r, and the number of populations n. Initial the ith bat position X_i^0 randomly by binary coding method, and initial the bat speed V_i^0 randomly.
Step (2): Calculate the initial fitness $f(X_i^0)$ of each bat, and find the bat position of the initial optimal fitness function, recorded as X_{best}^0.
Step (3): Update the pulse frequency vector F_i^k of the bat individual and the velocity vector V_i^k

$$F_i^k = F_{\min} + (F_{\max} - F_{\min})\beta \tag{12}$$

$$V_i^k = V_i^{k-1} + \left(X_i^k - X_{\text{best}}^{k-1}\right)F_i^k \tag{13}$$

where F_i^k is the pulse frequency of the ith bat at the kth iteration; $F_{\min}$ is minimum frequency; $F_{\max}$ is the maximum frequency; different pulse frequencies will increase the diversity of bats; $\beta \in [0,1]$ is to satisfy the uniform distribution The random number; F_i^k and X_i^k are the velocity and position of the ith bat at the kth iteration, respectively; X_{best}^k is the optimal position at the kth iteration.
Step (4): Calculate the speed conversion vector T_i^k for each bat;

$$T_i^k = \left|\frac{2}{\pi}\arctan\left(\frac{\pi}{2}V_i^k\right)\right| \tag{14}$$

Step (5): Update bat position.

$$X_{i,m}^{k-1} = \begin{cases} (X_{i,m}^{k-1})^{-1}, rand_1 < T_{i,m}^k \\ X_{i,m}^{k-1}, other \end{cases} \quad (15)$$

$$X_{i,m}^{k-1} = \begin{cases} X_{i,m}^{k-1}, r < rand_2 \\ X_{i,m}^{k-1}, other \end{cases} \quad (16)$$

where, $X_{i,m}^k$ is the value of the mth coded bit of the ith bat l at the kth iteration; $T_{i,m}^k$ is the velocity conversion of the mth coded bit of the ith bat at the kth iteration; $(.)^{-1}$ is inverse function; $rand_1$ and $rand_2$ are random numbers of [0, 1]; r is pulse frequency.
Step (6): Calculate the fitness value of all bats. If $rand_3$ < A and $f(X_i^k) < f(X_{best}^k)$, accept the value, otherwise retain the fitness value obtained from the last iteration calculation.
Step (7): The fitness values of the individual bat individuals are sorted to find the individual position X_{best}^k and the fitness value $f(X_{\mathrm{best}}^k)$ of the optimal fitness function at the current iteration.
Step (8): If the algorithm iteration does not reach the maximum number of iterations, return to Step (3), otherwise, output the optimal solution.

5.3 Stochastic Power Flow Calculation Method

In this paper, the uncertainty of EV and the timing characteristics of DG and conventional load are considered. In this paper, the stochastic power flow method based on Monte Carlo simulation (MCS) is used to solve the distribution network power flow with uncertain factors. According to the random sampling of the EV state at different times in the system, the corresponding state of the system is obtained by extracting the DG at different time and the output of the conventional load. Then the power distribution of each branch of the system is obtained by using the deterministic power flow calculation method to calculate the power loss target and so on [12].

6 Simulation Analysis

6.1 Simulation System Configuration

The method proposed in this paper is used to optimize the DG planning and configuration of the IEEE33 node distribution system. Installation cost of WT, PV, MT are 1400$/kW, 1800$/kW and 700$/kW, respectively; power loss price is 0.07 $/kWh; load and distributed power factor is 0.9; upper limit of total access capacity for DG is 380 kW. Suppose a total of 400 EVs in one day are connected to the area. All nodes in the distribution network have access to the DG conditions.

The population size of the algorithm is 25; the maximum number of iterations is 300, the penalty factor is $K = 100$; the sampling times of Monte Carlo is $N_{mcs} = 100$.

6.2 Clustering Processing Results of Load Time-Sequence Data

In this paper, the daily load curve data of a certain area in Guangdong Province, China are selected as clustering samples. The typical load sequence curve obtained by normalized clustering is shown in Fig. 2.

According to the analysis results, it can be seen that there are three typical load characteristics in this area. The load type of each node in the IEEE33 node system is set as follow: Type1: 4,10,11,13; Type2: 2,3,5,6,8,12,16,17,18,19,20,22, 23,29,30,32,33; Type 3: 7,9,14,15,21,24,25,26,27,28,31.

6.3 Simulation Results and Analysis

Comparison of Single-Objective and Multi-Objective Optimization Effects. The single-objective optimization of each objective and multi-objective optimization are carried out. The results are shown in Table 1. The distribution network loss target weight, each target weights are all taken as 1/3, that is, $\omega_1 = \omega_2 = \omega_3 = 1/3$.

It can be seen from the table that distribution network loss optimization results with the goal of minimum construction operation cost (i.e. no DG access) are higher than other optimization scenarios, which shows that the access of DG can effectively reduce the distribution network loss. In addition, compared with the single-objective optimization results for distribution network losses, the

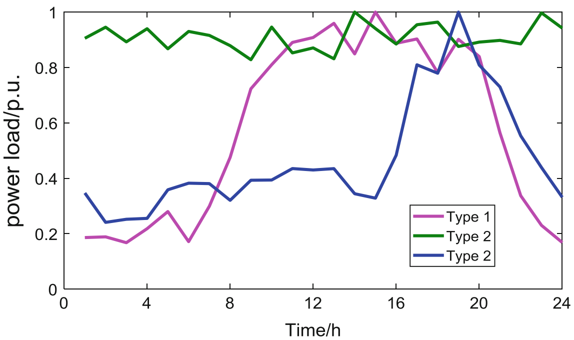

Fig. 2 Clustering results of load time series characteristics

Table 1 Results of single and multiple objectives optimizations

Target	Distribution network loss target/10^4\$	DG construction operation cost target/10^4\$	Environmental benefit target/ 10^4\$
Minimum network loss	5.74	17.39	6.27
Minimum construction operation cost (without DG access)	7.46	0	0
Maximum environmental benefit	6.03	27.11	9.64
Multiple target	6.21	19.02	8.77

optimization results of the multi-objective algorithm in this paper balance the objectives of all aspects, sacrificing a small amount of distribution network losses and DG construction operation costs. The goal of environmental benefit has been greatly raised. It is of great significance to improve the environmental quality and improve the living standard of the people in the planned area.

Analysis of Optimization Effect Under Different Target Weight Setting.

Case 1: the optimization target focuses on the social environmental protection benefits, and the weight setting of each goal is $\omega_1 = 0.4$; $\omega_2 = 0.1$; $\omega_3 = 0.5$;

Case2: the optimization goal focuses on the investment operation cost of the power supply enterprise, and its target weights are $\omega 1 = 0.4$; $\omega 2 = 0.5$; $\omega 3 = 0.1$.

The optimization results are shown in Tables 2, 3 and 4.

Comparison and analysis of overall optimization results. From the optimization results of Table 2, we can see that the network loss costs of the two optimization modes are 12.46 and 10.17% lower than those without DG access, respectively. This shows that reasonable DG access can effectively reduce the cost of network loss. In addition, two cases are compared and analyzed. Case 1 focuses on social environmental protection, and the environmental benefit is the highest in the optimization results, which is more than that of Case 2, but the construction and operation cost of DG is increased. Case 2 focuses on the investment operation cost of the power supply enterprise, and the construction operation cost of the optimization result is less than that of the case 1, but it is replaced by reducing the

Table 2 Optimization results comparison of different case

Case	Cost of network loss/10^4\$	Construction operation cost/10^4\$	Environmental benefits/10^4\$
Without DG access	7.46	0	0
1	6.53	11.60	4.27
2	6.70	9.38	3.37

Table 3 Configuration results of distributed generator optimization

Case1			Case2		
Node number	DG access Type	Access capacity /kW	Node number	DG access Type	Access capacity/kW
3	WT	50	12	PV	70
10	PV	30	13	WT	30
11	PV	50	15	PV	30
16	MT	40	17	PV	20
21	PV	30	21	MT	20
23	MT	20	26	PV	30
25	PV	30	30	WT	30
27	PV	40	31	PV	30
29	WT	60	33	MT	40
32	PV	30	–	–	–

Table 4 Access quantity and access proportion of distributed generation

Case1			Case2		
DG type	Access/kW	Access ratio (%)	DG type	Access/kW	Access ratio (%)
WT	110	28.95	WT	60	17.64
PV	210	55.26	PV	180	52.94
MT	60	15.79	MT	100	29.41
Total access	380	100	Total access	340	100

environmental benefit. This is because DG power generation has the characteristics of clean and environmental protection, DG access to the distribution network to replace the traditional coal-fired units to generate electricity, will improve the social and environmental benefits. However, the larger the DG access capacity, the higher the construction operation cost.

Comparison and analysis of the results of distributed generator configuration. It can be seen from the optimization results that the total access capacity of DG in the two schemes is 380 kW and 340 kW, respectively. In the optimization scheme, WG and PV access are the main ones, which is because the environmental benefit target is considered in the optimization goal, and the contribution of these two types of non-polluting DG to the environmental benefit is greater. In addition, in the two schemes, PV access is relatively stable. In case 2, compared with case 1, the proportion of WG access decreased from 28.95 to 17.64%, and the proportion of MT access increased from 15.79 to 29.41%. This is due to the fact that the cost of WG is higher than that of MT when it comes down When the objective weight of environmental benefit and the operation cost of DG are raised, the algorithm will adjust the configuration of distributed generator, reduce the access capacity of WG and PV, which contribute greatly to the environmental benefit, and increase the access ratio of MT.

7 Conclusion

The main work of this paper is summarized as follows:

(1) considering the uncertainty of EV access distribution network, the probability model of EV charging characteristics is established. In addition, the clustering method is used to extract the typical timing characteristics of distributed power supply and conventional load, which makes the planning model more close to the actual scene.
(2) A multi-objective DG optimal configuration model is established, which integrates the operation cost of DG construction, distribution network loss and environmental benefit cost. Planners can flexibly change the weights of different objectives according to the requirements of planning tasks, and obtain different optimal allocation results.
(3) using the binary bat algorithm to solve the programming model, the rationality and effectiveness of the proposed model and method are verified.

References

1. Cheng H, Hu X, Wang L et al (2019) Review on research of regional integrated energy system planning. Autom Electr Power Syst 43(7):2–13
2. Pan Z, Zhang X, Yu T et al (2017) Hierarchical real-time optimized dispatching for large-scale clusters of electric vehicles. Autom Electr Power Syst 41(16):96–104
3. Pan J, Wu H, Xu D et al (2019) Capacity optimization of rooftop photovoltaic based on photovoltaic/electric vehicle/load game. Autom Electr Power Syst 43(1):186–193
4. Hu Z, Luo H (2018) Research status and prospect of automatic generation control with integration of large-scale renewable energy. Autom Electr Power Syst 42(8):2–15
5. Zhu J, Wei G, Lou G et al (2017) Learning automata-based methodology for optimal allocation of renewable distributed generation considering network reconfiguration. IEEE Access 5(99):14275–14288
6. Dugan RC, Mcdermott TE, Ball GJ (2001) Planning for distributed generation. IEEE Ind Appl Mag 7(2):80–88
7. Huang X (2018) Capacity optimization of distributed generation for stand-alone microgrid considering controllable load. Proc CSEE 38(07):1962–1970
8. U.S. Department of transportation, federal highway administration [DB/OL]. National household travel survey, 2009. http://nhts.ornl.gov

9. Yang Z, Lin X, Jiang W et al (2017) An electricity data cluster analysis method based on SAGA-FCM algorithm. In: IEEE International Conference on Networking. IEEE
10. Qian K (2008) Environmental benefits analysis of distributed generation. Proc CSEE 28 (29):11–15
11. Mirjalili S, Mirjalili SM, Yang XS (2014) Binary bat algorithm. Neural Comput Appl 25(3–4):663–681
12. Peng X, Lin L, Liu Y et al (2015) Optimal distributed generator allocation method based on correlation latin hypercube sampling monte carlo simulation embedded crisscross optimization algorithm. Proc CSEE 35(16):4077–4085